

Cambridge Centre for Computational Chemical Engineering

University of Cambridge

Department of Chemical Engineering

Preprint

ISSN 1473 – 4273

First-principles thermochemistry for the production of TiO₂ from TiCl₄

Richard H. West, Gregory J. O. Beran, Willam H. Green¹,

Markus Kraft²

submitted: October 8, 2006

¹ Department of Chemical Engineering
Massachusetts Institute of Technology
77 Massachusetts Avenue, 66-270A
Cambridge, MA 02139
USA
E-mail: whgreen@mit.edu

² Department of Chemical Engineering
University of Cambridge
Pembroke Street
Cambridge CB2 3RA
UK
E-mail: mk306@cam.ac.uk

Preprint No. 42



c4e

Key words and phrases. Titania, titanium tetrachloride, thermochemistry, density functional theory (DFT).

Edited by

Cambridge Centre for Computational Chemical Engineering
Department of Chemical Engineering
University of Cambridge
Cambridge CB2 3RA
United Kingdom.

Fax: + 44 (0)1223 334796

E-Mail: c4e@cheng.cam.ac.uk

World Wide Web: <http://www.cheng.cam.ac.uk/c4e/>

Abstract

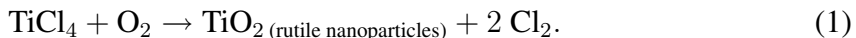
Despite the industrial importance of the process, detailed chemistry of the high temperature oxidation of titanium tetrachloride (TiCl_4) to produce titania (TiO_2) nanoparticles remains unknown, partly due to a lack of thermochemical data. This work presents the thermochemistry of many of the intermediates in the early stages of the mechanism, computed using quantum chemistry. The enthalpies of formation and thermochemical data for TiOCl , TiOCl_2 , TiOCl_3 , TiO_2Cl_2 , TiO_2Cl_3 , $\text{Ti}_2\text{O}_2\text{Cl}_3$, $\text{Ti}_2\text{O}_2\text{Cl}_4$, $\text{Ti}_2\text{O}_3\text{Cl}_2$, $\text{Ti}_2\text{O}_3\text{Cl}_3$, $\text{Ti}_3\text{O}_4\text{Cl}_4$, and $\text{Ti}_5\text{O}_6\text{Cl}_8$ were calculated using density functional theory (DFT). Use of isodesmic and isogyric reactions was shown to be important for determining standard enthalpy of formation ($\Delta_f H_{298\text{ K}}^\circ$) values for these transition metal oxychloride species. TiOCl_2 , of particular importance in this mechanism, was also studied with CCSD(T) and found to have $\Delta_f H_{298\text{ K}}^\circ = -598 \pm 20 \text{ kJ/mol}$. Finally, equilibrium calculations are performed to try to identify which intermediates are likely to be most prevalent in the high temperature industrial process, and as a first attempt to identify the size of the critical nucleus.

Contents

1	Introduction	3
2	Methods	4
2.1	Quantum Calculations	4
2.2	Frequency Scaling	5
2.3	Statistical Mechanics and Equilibrium Composition	6
2.4	Enthalpies of formation: Isodesmic and Isogyric Reactions	7
3	Results and Discussion	8
3.1	Geometries	8
3.2	Atomization Energies	9
3.3	TiOCl ₂	11
3.4	Thermochemistry	12
3.5	Equilibrium Composition	14
4	Conclusion	15
5	Acknowledgements	15
6	Appendices	19

1 Introduction

Titanium dioxide is currently produced at a rate over 4 million tons per year; half is used in paint, a quarter in plastics such as carrier bags and refrigerator doors, and most of the rest in paper, synthetic fibres and ceramics. It is also used as a catalyst support and photocatalyst. The preferred production method is the chloride process, during which purified titanium tetrachloride is oxidized at high temperatures (1500–2000 K) in a pure oxygen plasma or flame to produce TiO_2 nanoparticles. The overall stoichiometry of this oxidation process is:



Although the chloride process is a mature technology, which has been used in industry since 1958, understanding of the gas-phase reactions of TiCl_4 oxidation remains incomplete [21].

Over the years, various mechanisms have been proposed to describe TiCl_4 oxidation. Pratsinis *et al.*[32] proposed a mechanism in which TiCl_4 decomposes to TiCl_z radicals ($z < 4$) via thermal decomposition and abstraction reactions. These radicals are then oxidized to various TiO_yCl_z oxychlorides ($y \leq 2$, $z < 4$). The oxychlorides then dimerize to form $\text{Ti}_x\text{O}_y\text{Cl}_z$ ($x = 2$, $y \leq 4$) before reacting to yield species with $x > 2$, with subsequent reactions resulting in $(\text{TiO}_2)_n$ nanoparticles ($n \gg 100$). Like Pratsinis, Karlemo *et al.*[21] proposed a mechanism via oxychloride intermediates, specifically TiOCl_2 , which they found in detectable quantities. Despite these proposed mechanisms, no detailed simulations have been attempted due to a lack of thermochemical data for the intermediate species.

Experimentally, the only oxychloride intermediate to have been observed directly is TiOCl_2 [19, 21]; its presence at detectable levels suggests that it is likely to play an important role in the mechanism. Yet, the only thermochemical data currently available for TiOCl_2 and TiOCl , which are from the NIST JANAF Thermochemical Tables[7], were estimated in 1963. Other reactive intermediates in the chloride process are even more poorly characterized. Given that current experimental techniques cannot easily provide detailed thermochemical information for such short-lived reactive intermediates, quantum calculations provide a useful complementary tool.

Quantum calculations have previously been applied to titanium oxide species, particularly in the context of nanoclusters. Albaret *et al.*[2] have studied $\text{Ti}_n\text{O}_{2n+m}$ clusters ($n = 1..3$, $m = 0, 1$) using pseudopotential plane-wave density functional theory (DFT), and Woodley *et al.*[37] recently used DFT to study the minimum energy structures of small $(\text{TiO}_2)_n$ clusters ($n = 1..8$). While these studies shed light on the electronic and structural properties of titania nanoclusters, chlorine-free molecules are not part of the mechanisms proposed by Pratsinis or Karlemo, and are unlikely to play an important role as intermediates in the chloride process[21, 32].

The aim of this work is to provide thermochemical data for some of the titanium oxychloride species ($\text{Ti}_x\text{O}_y\text{Cl}_z$), which will enable the development of more detailed kinetic

models of the combustion of titanium tetrachloride. The results from three DFT functionals are compared, giving some indication of the reliability of DFT for these transition metal oxychloride species.

As well as probably playing an important role in the TiCl_4 oxidation mechanism, TiOCl_2 is a useful reference species for calculating the enthalpies of many other species; it is therefore subjected to a more detailed analysis using coupled cluster CCSD(T), often called “the gold standard of quantum chemistry”.

Since the optical and catalytic properties of TiO_2 depend strongly on particle size, a major technological issue in this large-scale industrial process is precisely controlling the particle size distribution. The size distribution is expected to depend strongly on the particle nucleation rate, which is strongly related to the size of the critical nucleus. Here we perform equilibrium calculations to try to identify which intermediates are likely to be most prevalent in the high temperature industrial process, and as a first attempt to identify the size of the critical nucleus.

2 Methods

2.1 Quantum Calculations

Molecular geometries have been optimized and analytical harmonic frequencies calculated using three different DFT functionals: mPW91[1, 28, 29], B3LYP[4], and B97-1[14] as recommended by Boese *et al.* [6]. All functionals were as implemented in the Gaussian 03 program package[8].

Jeong et al. [20] chose to use the B3P86 functional for determining energies of atomization in a study of Ti_xO_y molecules, observing that gradient-corrected hybrid exchange correlation functionals were useful for this system, and the P86 functional seemed to work better than for example PW91. The most widely used DFT functional is currently the gradient-corrected hybrid functional B3LYP. Boese et al. [6] suggest the continued popularity of this and other first-generation functionals rather than the more accurate second-generation functionals may be due to sheer user inertia. They recommend the second generation hybrid functional B97-1 as probably the best choice when it comes to using density functional hybrid calculations. Woodley et al. [37] used the reparameterisation of this, B97-2, when optimising small $(\text{TiO}_2)_n$ clusters.

The basis set for all reported DFT calculations was 6-311+G(d,p)[8]. This consists of the 6-311G basis set[22] for oxygen; the McLean-Chandler (12s,9p) (621111,52111) “negative ion” basis set [25] for chlorine; the Wachters-Hay all-electron basis set[15, 35] for titanium, using the scaling factors of Raghavachari and Trucks[33]; and supplementary polarization functions (one *d* function each for O and Cl, and one *f* function for Ti, since *d* functions are already present in the latter) and diffuse functions (one *s* and one *p* on all three atoms, plus an additional *d* diffuse function on Ti). Such a supplemented, triple-zeta basis set should be large enough to ensure that the basis set truncation error is comparable with, or smaller than, the inherent errors in the DFT[6].

Some species, such as TiOCl_3 , could not be adequately described by the default settings in Gaussian, so the B3LYP and B97-1 calculations were repeated with less restrictive settings: spin restrictions were removed to detect possible spin contamination in singlet species, symmetry constraints were lifted allowing symmetry-breaking Jahn-Teller type distortions, the integral grid was increased to a pruned (99,590) grid¹ and the geometry optimisation convergence criteria were tightened.²

To establish the spin multiplicity of the ground state, the lowest-energy state of different spin multiplicity was also calculated in many cases. Although not demonstrated in the case of TiCl_4 oxidation, the kinetic role of electronically excited species is important in some other combustion systems[26]. This may be the case in TiCl_4 oxidation since the temperature in the process is high (about 1800 K). Therefore we report here the the lowest-energy state of different spin multiplicity in addition to the ground state. Excited states with the same spin multiplicity as the ground state were not considered.

Species required to evaluate the enthalpy of formation of TiOCl_2 were investigated in more detail. Geometry optimisation and frequency analyses were performed with BPW91[3, 28, 29] and PW91PW91[28, 29] in addition to the three DFT functionals described above. Using B3LYP optimized geometries, single point coupled cluster CCSD(T) calculations were performed using the software GAMESS-UK version 7[13, 23]. This software can only perform spin restricted CCSD(T) calculations; however, this is not a problem in this case as none of the species studied with CCSD(T) preferred a spin unrestricted solution at the UB3LYP or UHF levels of theory.

Three different basis sets were used for the CCSD(T) calculations. For titanium the two smallest basis sets both used the LANL2 Hay and Wadt Effective Core Potentials (ECPs), with the inner-valence forms used for transition metals[16]. Oxygen and chlorine were taken from 3-21G [5, 10] for the smallest basis set and 6-311G[22] for the intermediate case. For the largest basis set calculations, the all-electron 6-311+G(d,p) basis set was used for all three elements, as with the DFT calculations. Only three small molecules (TiCl_4 , TiO_2 and TiOCl_2) were calculated with the larger two basis sets due to the n^7 scaling of CCSD(T) and the limited computing resources available.

Vibrational frequencies were not calculated at the HF, MP2, CCSD or CCSD(T) levels so these enthalpies have been corrected with thermal contributions according to B97-1/6-311+G(d,p) frequencies and rotational constants.

2.2 Frequency Scaling

As explained by Scott and Radom [34], scaling factors designed to predict frequencies in their own right are not optimal for predicting thermodynamic properties derived from those frequencies. [34] provides suitable scaling factors for a variety of quantum calculation methods and basis sets, derived by minimising the least squares error in the thermal

¹Gaussian keyword `Integral(Grid=UltraFine)`.

²Gaussian keyword `opt=(Tight)`. Criteria: maximum force $< 1.5 \times 10^{-5}$, RMS force $< 1 \times 10^{-5}$, maximum displacement $< 6 \times 10^{-5}$, RMS displacement $< 4 \times 10^{-5}$.

contribution to H and S . To estimate the appropriate scaling factors for basis sets not studied by Scott and Radom, a relationship was derived by comparing Scott and Radom's scaling factors to those for the same methods and basis sets in the NIST CCCBDB[27] database (Figure 1). This method was used to calculate a scaling factor of 1.01 for thermodynamic properties derived from B3LYP/6-311G(d,p) calculations (without the diffuse functions). No recommended scaling factors for B97-1 or B3LYP/6-311+G(d,p) (with diffuse functions) could be found, so the frequencies were left unscaled. Because the recommended scaling for B3LYP/6-311G(d,p) is so close to 1.0, it is unlikely that significant errors will be introduced by leaving the frequencies unscaled.

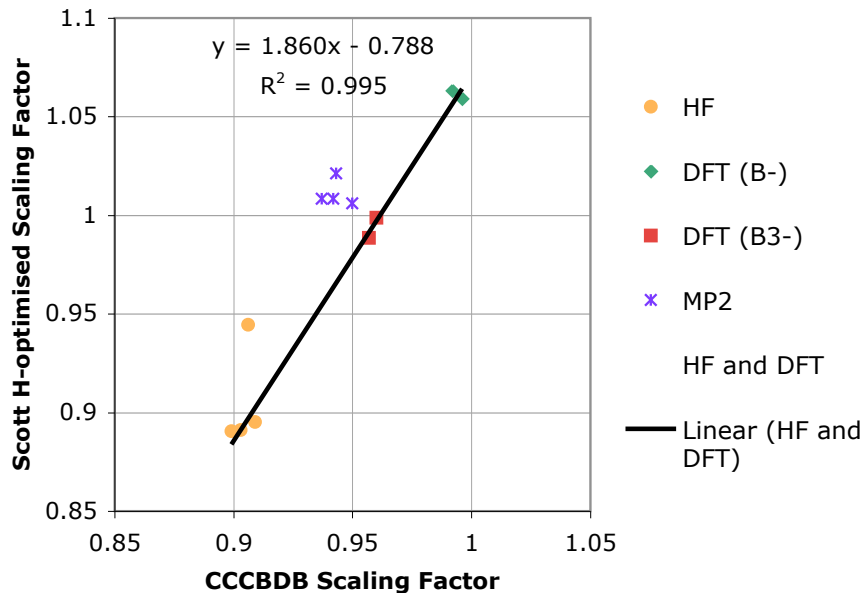


Figure 1: Scaling factors applicable for calculation of thermal contributions to $\Delta_f H_{298\text{ K}}^\circ$ recommended by [34] plotted against scaling factors from the CCCBDB. The linear relationship shown was used to estimate suitable scaling factors based on the CCCBDB.

2.3 Statistical Mechanics and Equilibrium Composition

Heat capacities (C_p), integrated heat capacities ($H(T) - H(0\text{ K})$) and entropies (S) were calculated for temperatures in the range 100–3000 K using the rigid rotator harmonic oscillator (RRHO) approximation, taking unscaled vibrational frequencies and rotational constants from the B97-1 calculations (see Tab. 4).

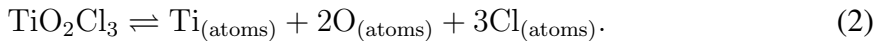
Polynomials in the NASA form [11] were fitted to $C_p(T)/R$, H° and S° over the temperature ranges 100–1000 K and 1000–3000 K, constrained to ensure $C_p(T)$ and its first two derivatives matched at 1000 K. Using the fitted polynomials for $C_p(T)$, $H^\circ(T)$ and $S^\circ(T)$, the equilibrium composition as a function of temperature was calculated using the open source software Cantera[9].

2.4 Enthalpies of formation: Isodesmic and Isogyric Reactions

The atomization energies reported in Section 3.2 were found by subtracting the DFT-computed absolute energies of the component atoms in isolation, from the absolute energies of the species computed at the same level of theory. Standard enthalpies of formation ($\Delta_f H_{298\text{ K}}^\circ$) are found by relating the computed absolute enthalpies of the unknown species to those of other reference species with previously known standard enthalpies. Although a common choice for these reference species are the isolated atoms, this can lead to systematic errors in the DFT propagating to the final enthalpies; better results can usually be obtained using reference species that are more similar in terms of electronic structure to the unknown species.

Ideally the reference species are chosen such that they are linked to the unknown species via an isodesmic reaction, in which the type of the bonds broken are the same as the type of bonds formed. Because the products and reactants have similar electronic structures, systematic errors in the DFT are largely cancelled out[17]. While less desirable than isodesmic reactions, isogyric reactions, which conserve the number of electron pairs in reactants and products, are still better than using atomization reactions[30, 31].

Reaction choice is particularly important with the titanium oxychloride species, as shown here with the radical TiO_2Cl_3 . Calculation of standard enthalpy of formation from atomization energies is equivalent to using the reaction



Here a doublet reactant (one unpaired electron) is compared to three triplet and three doublet species (total of nine unpaired electrons). Using this reaction to establish the standard enthalpy of formation, with the 6-311+G(d,p) basis set, the mPWPW91, B3LYP and B97-1 functionals give formation enthalpies for TiO_2Cl_3 of -865 , -612 and -694 kJ/mol respectively. This is a spread of 253 kJ/mol, far exceeding the expected accuracy of DFT calculations[6].

Reliable enthalpies of formation are available for TiCl_3 and O_2 , therefore an alternative choice of reaction is



However, on the left hand side is a doublet with the spin concentrated on the oxygen atoms, which are in the 2– oxidation state, and on the right is one doublet with the spin on the titanium and one triplet with the oxygen atoms in the ground oxidation state. Using this scheme to establish enthalpies changes the mPWPW91 value to -702 kJ/mol, a change of 163 kJ/mol relative to the atomization scheme. The B3LYP and B97-1 functionals give -648 and -657 kJ/mol respectively, reducing the overall spread to 54 kJ/mol.

A third alternative reaction is



This reaction is isogyric, as there are 61 electron pairs and one unpaired electron on both the reactant and product sides, with one doublet and one singlet on each side of the reaction. Linking the absolute energies to standard values with this isogyric reaction places

the standard enthalpy of formation of TiO_2Cl_3 at -734 , -772 and -771 kJ/mol according to the mPW91, B3LYP and B97-1 functionals respectively. The overall spread of 38 kJ/mol and the very close agreement of the latter two functionals adds confidence to the numbers achieved this way. The variation of up to 160 kJ/mol between reaction schemes shows both the importance of their choice and the challenge of obtaining a uniformly accurate treatment of these transition metal species with different spin states[12].

Due to the paucity of thermochemical data for transition metal oxychloride species, it was not possible to find isodesmic or isogyric reactions linking the species studied in this work to species with reliable literature values for $\Delta_f H_{298\text{ K}}^\circ$. However, any reaction that leaves some bonds intact is preferable to atomization. The reactions used to evaluate standard enthalpies of formation are shown in Table 1.

Table 1: Reactions used to evaluate standard enthalpies of formation ($\Delta_f H_{298\text{ K}}^\circ$) from computed absolute enthalpies.

species	type	reaction
TiOCl	isodesmic	$\text{TiOCl}_2^a + \text{TiCl}_3^b \rightleftharpoons \text{TiOCl} + \text{TiCl}_4^c$
TiOCl_2	isogyric	$\frac{1}{2} \text{TiCl}_4^c + \frac{1}{2} \text{TiO}_2^c \rightleftharpoons \text{TiOCl}_2$
TiOCl_3	anisogyric	$\text{TiCl}_4^c + \text{TiOCl}_2^a \rightleftharpoons \text{TiOCl}_3 + \text{TiCl}_3^b$
TiO_2Cl_3	isogyric	$\text{TiCl}_4^c + \text{OCLO}^c \rightleftharpoons \text{TiO}_2\text{Cl}_3 + \text{Cl}_2^c$
TiO_2Cl_2	anisogyric	$\text{TiCl}_2^b + \text{O}_2^c \rightleftharpoons \text{TiO}_2\text{Cl}_2$
$\text{Ti}_2\text{O}_2\text{Cl}_4$	isogyric	$2 \text{TiOCl}_2^a \rightleftharpoons \text{Ti}_2\text{O}_2\text{Cl}_4$
$\text{Ti}_2\text{O}_2\text{Cl}_3$	isogyric	$2 \text{TiOCl}_2^a + \text{TiCl}_3^b \rightleftharpoons \text{Ti}_2\text{O}_2\text{Cl}_3 + \text{TiCl}_4^c$
$\text{Ti}_2\text{O}_3\text{Cl}_3$	anisogyric	$3 \text{TiOCl}_2^a \rightleftharpoons \text{Ti}_2\text{O}_3\text{Cl}_3 + \text{TiCl}_3^b$
$\text{Ti}_2\text{O}_3\text{Cl}_2$	isogyric	$2 \text{TiOCl}_2^a + \text{TiOCl}_2^a \rightleftharpoons \text{Ti}_2\text{O}_3\text{Cl}_2 + \text{TiCl}_4^c$
$\text{Ti}_3\text{O}_4\text{Cl}_4$	isogyric	$2 \text{TiOCl}_2^a + \text{TiO}_2^b \rightleftharpoons \text{Ti}_3\text{O}_4\text{Cl}_4$
$\text{Ti}_5\text{O}_6\text{Cl}_8$	isogyric	$6 \text{TiOCl}_2^a \rightleftharpoons \text{Ti}_5\text{O}_6\text{Cl}_8 + \text{TiCl}_4^c$

^a Enthalpy of formation from this work.

^b Enthalpy of formation from Hildenbrand (1996)[18]

^c Enthalpy of formation from NIST-JANAF tables [7]

3 Results and Discussion

3.1 Geometries

Figure 2 shows the molecular geometries of the ground state of each molecule after optimisation with B97-1/6-311+G(d,p).

At this level of theory, TiOCl_3 in a C_{3v} conformation has an imaginary frequency. This

is due to a Jahn-Teller distortion, which results from a very low-lying first excited state (0.21 eV for the C_{3v} structure according to TDDFT with the B3LYP functional). The C_s geometry reported here is stable at this level of theory.

Two stable geometries for TiO_2Cl_2 were located. At the B97-1/6-311+G(d,p) level the isomer with a trigonal Ti center and a dangling $-O-O-$ has an electronic energy 201 kJ/mol higher than the structure with the distorted tetrahedral geometry reported here where the O atoms are both bonded to the Ti.

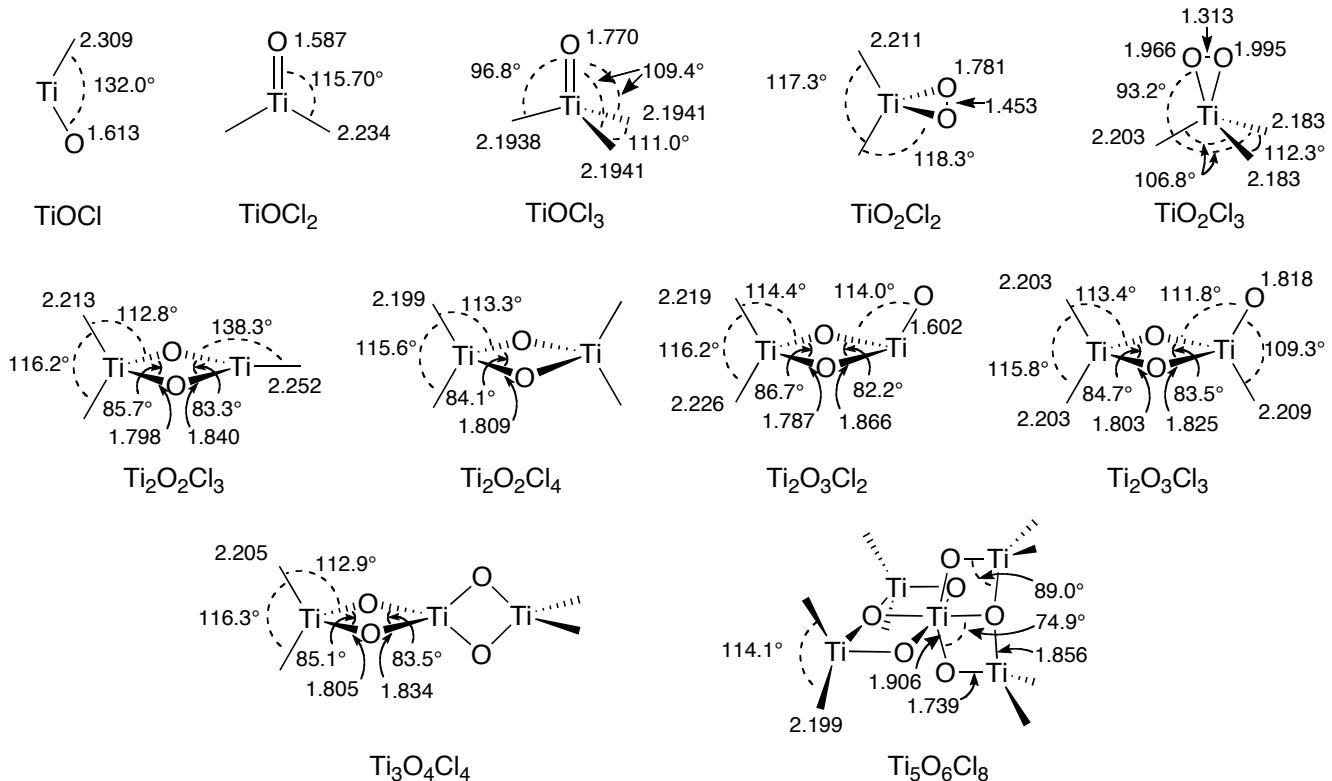


Figure 2: Molecular geometries after optimisation with B97-1/6-311+G(d,p). Bond lengths are in Ångströms, and unlabelled atoms are chlorine.

3.2 Atomization Energies

Although we have not used atomization reactions to calculate enthalpies of formation, we report atomization energies here to facilitate reproduction of our results. Table 2 shows the atomization energies for the ground electronic state calculated with the 6-311+G(d,p) basis set using three DFT functionals: mPW91, B3LYP, and B97-1.

The lowest-energy states of different spin multiplicity from the ground states were of considerably higher energies. The smallest gap was for $TiCl$ in which the doublet state is ~ 40 kJ/mol higher than the quartet state; all the other gaps were at least 100 kJ/mol.

Table 2: Atomization Energies at 0 K in kJ/mol with 6-311+G(d,p) basis set. DFT calculations include ZPE correction.

species	spin state	mPWPPW91	B3LYP	B97-1	Literature
TiO ₂	Singlet	-1436	-1226	-1269	-1268 ^a
	Triplet				-
TiCl ₄	Singlet	-1828	-1641	-1719	-1687 ^a
	Triplet			-	-
TiCl ₃	Doublet	-1424	-1296	-1354	-1335 ^b
	Quartet			-	-
TiCl ₂	Triplet	-974	-840	-921	-913 ^b
	Singlet				-
TiCl	Quartet	-481	-428	-438	-405 ^b
	Doublet				-
TiOCl	Doublet	-1231	-1085	-1127	-1074 ^a
	Quartet				-
TiOCl ₂	Singlet	-1675	-1490	-1552	-1489 ^a
	Triplet				-
TiOCl ₃	Doublet	-1838	-1627	-1694	-
	Quartet				-
TiO ₂ Cl ₂	Singlet	-1953	-1715	-1785	-
	Triplet			-	-
TiO ₂ Cl ₃	Doublet	-2188	-1935	-2018	-
	Quartet				-
Ti ₂ O ₂ Cl ₄	Singlet	-3705	-3335	-3457	-
	Triplet				-
Ti ₂ O ₂ Cl ₃	Doublet	-3281	-2960	-3061	-
	Quartet				-
Ti ₂ O ₃ Cl ₂	Singlet	-3515	-3133	-3238	-
	Triplet				-
Ti ₂ O ₃ Cl ₃	Doublet	-3697	-3300	-3421	-
	Quartet				-
Ti ₃ O ₄ Cl ₄	Singlet	-5558	-5001	-5167	-
	Triplet				-
Ti ₅ O ₆ Cl ₈	Singlet	-	-8481	-8771	-
	Triplet	-	-	-	-

^a NIST-JANAF tables [7]

^b Atomization enthalpy at 298 K based on Hildenbrand[19] and the NIST-JANAF tables [7]

3.3 TiOCl₂

As explained in the introduction, TiOCl₂ and the species required to find its enthalpy of formation (TiCl₄ and TiO₂), were subjected to a more detailed analysis using two additional DFT functionals as well as HF, MP2 and coupled cluster calculations. The enthalpies of formation derived from these calculations are reported in Table 3.

Table 3: Enthalpies of formation of TiOCl₂ derived from the isogyric reaction described in Table 1. HF, MP2, CCSD and CCSD(T) calculations were based on B3LYP/6-311+G(d,p) geometries and have been corrected for thermal contributions to enthalpy using B97-1/6-311+G(d,p) frequencies.

basis set	method	$\Delta_f H_{298K}^\circ$ ^a
	Literature ^b	-546
LANL2 & 3-21G	HF	-652
	MP2	-635
	CCSD	-636
	CCSD(T)	-620
LANL2 & 6-311G(d,p)	HF	-636
	MP2	-623
	CCSD	-623
	CCSD(T)	-609
6-311+G(d,p)	PW91PW91	-578
	BPW91	-579
	mPWPW91	-579
	B3LYP	-590
	B97-1	-591
	HF	-638
	MP2	-607
	CCSD	-610
	CCSD(T)	-598

^a kJ/mol

^b NIST/JANAF tables[7]

The MP2/CCSD/CCSD(T) results converge nicely with respect to basis set and increasing level of correlation treatment. CCSD and MP2, which both include up to double excitations from the HF reference, agree very closely, lowering the enthalpy by 28–31 kJ/mol relative to HF/6-311+G(d,p). The additional perturbative inclusion of triple excitations in CCSD(T), though important, introduces a smaller correction, changing the energy by 9–12 kJ/mol from MP2 and CCSD in the 6-311+G(d,p) basis set. These results suggest that

the correlation treatment is well-behaved with respect to systematic improvement, and it seems reasonable to expect that higher order excitations would not alter the enthalpy of formation by more than ~ 10 kJ/mol. The good agreements with B3LYP and B97-1 (8 and 7 kJ/mol lower, respectively) further inspire confidence in the predictions within this basis set.

Although a supplemented triple-zeta basis set is sufficient for DFT calculations[6], it is possible that the CCSD(T) calculations are limited by basis set truncation error and would benefit from a larger basis set. Moving O and Cl from 3-21G, a poor double-zeta basis set, to 6-311G(d,p), a better triple-zeta basis set with polarization functions, lowers the enthalpy of TiOCl_2 by 11 kJ/mol for CCSD(T). A further 11 kJ/mol change occurs when the all-electron triple-zeta basis is used instead of the ECP for Ti and diffuse functions are added to all atoms. These relatively small changes in enthalpy suggest that basis set errors are not too large.

Based on these calculations we recommend a value of $\Delta_f H_{298\text{ K}}^\circ = -598 \pm 20$ kJ/mol for TiOCl_2 . The NIST/JANAF value of -546 kJ/mol, which apparently is an old estimate not based on any direct measurement, lies outside our estimated uncertainty, and so should be considered for revision. We have used the value calculated here (-598 kJ/mol) in deriving $\Delta_f H_{298\text{ K}}^\circ$ values for other species in this paper.

3.4 Thermochemistry

The recommended standard entropies and enthalpies of formation at 298 K are given in table 4 along with B97-1 frequencies. With the exception of TiOCl_2 the recommended enthalpies are based on the B97-1 functional, which is probably the most accurate[6]. For TiOCl_2 the electronic energy is from the CCSD(T)/6-311+G(d,p) calculation based on the B3LYP geometry, with the thermal energy based on B97-1 frequencies reported here.

For most species the enthalpies derived from B3LYP calculations differed from the B97-1 enthalpies by less than 2 kJ/mol. The exceptions were the three species that were evaluated through anisodesmic reactions: TiOCl_3 , TiO_2Cl_2 , and $\text{Ti}_2\text{O}_3\text{Cl}_3$, for which the B3LYP enthalpies were respectively 15 kJ/mol lower, 22 kJ/mol higher, and 7 kJ/mol lower than the B97-1 enthalpies. While this close agreement increases confidence in the calculations, it is worth remembering that the actual error will be larger than this; B3LYP and B97-1 are both hybrid DFT functionals with some exact (HF) exchange so behave similarly. MPWPW91, a pure DFT functional, gives enthalpies that differ from B97-1 by ~ 20 kJ/mol on average and as much as 59 kJ/mol for the anisodesmic reaction to find TiO_2Cl_2 . In addition to errors in the DFT calculations, errors in the reference species enthalpies will propagate to the enthalpies that are derived from them.

Table 4: Calculated thermochemistry at 298 K.

species	$\Delta_f H_{298\text{ K}}^\circ$ kJ/mol	$S_{298\text{ K}}^\circ$ J/mol K	rot. const. GHz	vibrational frequencies cm ⁻¹
TiOCl	-274 ^a	292	39.120 2.9782 2.7676	113 398 1036
TiOCl ₂	-598 ^b	335	5.4126 1.7850 1.3423	23.0 113 212 378 506 1091
TiOCl ₃	-639	379	1.6461 1.5723 1.0712	77.1 94.0 116 144 155 378 469 483 669
TiO ₂ Cl ₂	-558	342	2.6652 1.8968 1.1982	110 125 149 174 384 493 658 683 966
TiO ₂ Cl ₃	-774	404	1.2747 1.2687 1.1039	33.0 108 127 140 147 160 389 405 470 493 549 1229
Ti ₂ O ₂ Cl ₃	-1257	438	1.7164 0.4549 0.3859	14.1 72.4 82.7 100 140 161 273 278 393 422 495 539 695 708 760
Ti ₂ O ₂ Cl ₄	-1552	449	0.9517 0.4544 0.3262	40.4 65.8 91.6 97.1 102 116 152 214 294 302 398 410 489 527 539 710 731 767
Ti ₂ O ₃ Cl ₂	-1331	402	1.6100 0.7549 0.5699	59.6 101 122 142 164 256 303 335 462 488 494 707 722 776 1065
Ti ₂ O ₃ Cl ₃	-1418	461	1.2145 0.5034 0.3813	44.0 61.3 89.0 105 108 135 159 187 293 315 330 420 504 533 690 703 732 765
Ti ₃ O ₄ Cl ₄	-2301	538	0.8631 0.1581 0.1581	30.3 31.9 50.6 85.3 85.9 87.8 108 138 140 163 235 239 290 291 354 439 439 444 507 508 534 709 714 717 739 765 778
Ti ₅ O ₆ Cl ₈	-4011	823	0.1297 0.0875 0.0875	19.4 20.8 20.8 28.5 28.5 39.0 58.0 61.9 67.8 77.8 80.7 83.8 83.8 99.3 109 109 110 129 140 141 141 220 223 223 246 246 283 321 327 327 331 371 383 429 429 484 486 486 494 499 510 510 521 555 626 754 754 823 876 881 881

^a JANAF value: -244 kJ/mol (estimated in 1963).

^b Electronic energy from CCSD(T)/6-311+G(d,p) at B3LYP/6-311+G(d,p) geometry.
Thermal contribution to enthalpy from B97-1/6-3111+G(d,p) frequencies.
JANAF value: -546 kJ/mol (estimated in 1963).

3.5 Equilibrium Composition

Figure 3 shows the computed equilibrium composition of a gas initially comprising a stoichiometric mixture of TiCl_4 and O_2 , at a pressure of 3 bar, similar to that of the industrial process, and temperatures between 100 and 3000 K. The thermochemical data for TiOCl , TiOCl_2 , TiOCl_3 , TiO_2Cl_2 , TiO_2Cl_3 , $\text{Ti}_2\text{O}_2\text{Cl}_3$, $\text{Ti}_2\text{O}_2\text{Cl}_4$, $\text{Ti}_2\text{O}_3\text{Cl}_2$, $\text{Ti}_2\text{O}_3\text{Cl}_3$, $\text{Ti}_3\text{O}_4\text{Cl}_4$, and $\text{Ti}_5\text{O}_6\text{Cl}_8$, were taken from this work. Those for TiCl_4 , TiCl_3 , TiCl_2 , TiCl , Ti , TiO , TiO_2 , O , O_2 , O_3 , Cl , ClO , ClO_2 , Cl_2O were taken from the NASA database[11, 24] supplied with Cantera. All other species, including solid TiO_2 , were excluded from the simulation.

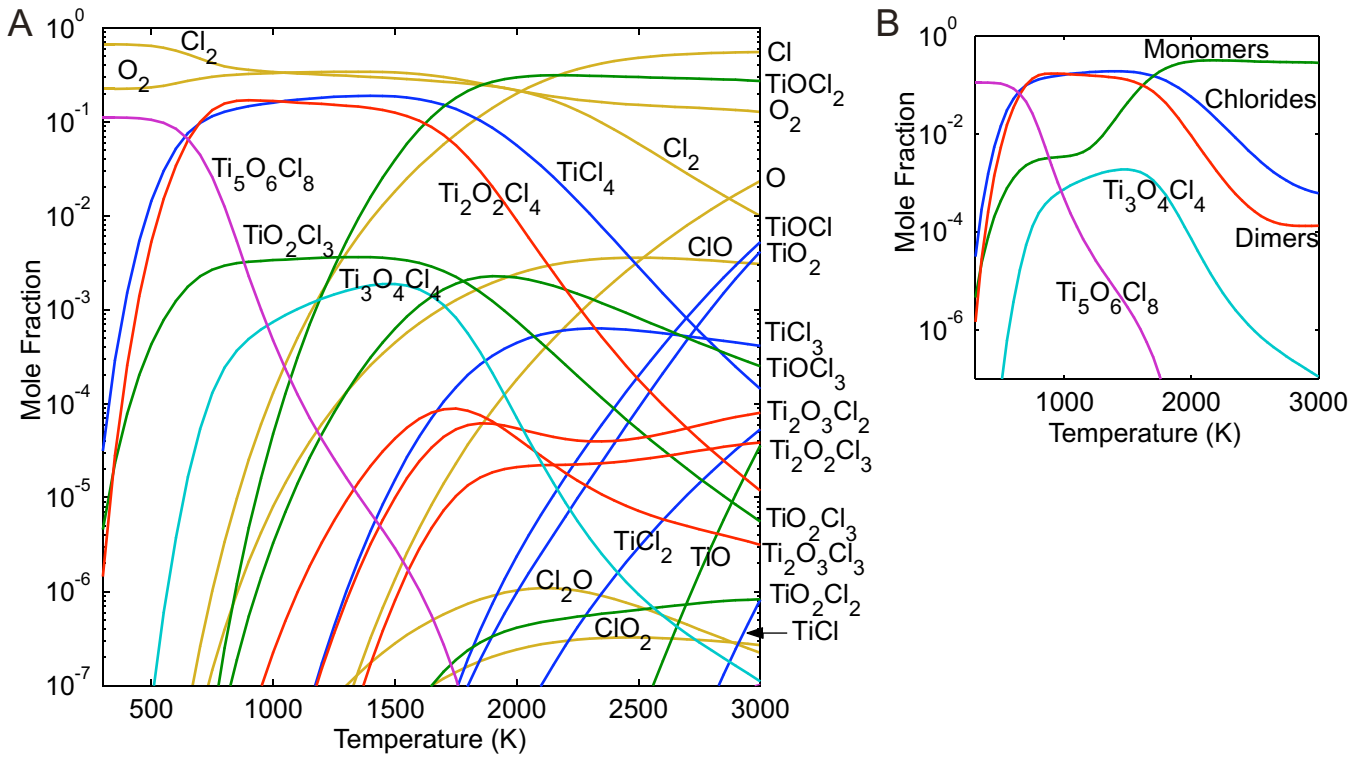


Figure 3: Computed equilibrium composition of a mixture initially containing 50 mol% TiCl_4 in O_2 , at 3 bar and 300–3000 K. (A) Detailed composition. (B) Summary with chlorides (TiCl_z), monomers (TiO_yCl_z), and dimers ($\text{Ti}_2\text{O}_y\text{Cl}_z$) grouped.

As anticipated, TiOCl_2 has the highest equilibrium concentration of all Ti_1 species except, below 2400 K, for the reactant TiCl_4 . Although less stable than TiOCl_2 , the other TiO_yCl_z species are no less important for the kinetic mechanism, because TiOCl_2 is unlikely to be formed directly from TiCl_z radicals, instead proceeding via TiO_2Cl_2 or TiO_2Cl_3 from reaction with O_2 , or via TiOCl_3 from reaction with ClO . Due to the stability of TiOCl_2 relative to other reactive Ti_1 species, the most likely collision that leads to a Ti_2 species is between two TiOCl_2 molecules. The product of TiOCl_2 dimerisation, $\text{Ti}_2\text{O}_2\text{Cl}_4$, is stable relative to the monomer at all temperatures below 2400 K, and is therefore likely to play an important role in the mechanism. $\text{Ti}_2\text{O}_2\text{Cl}_4$ can undergo chlorine abstraction and oxidation reactions to form other Ti_2 intermediates such as $\text{Ti}_2\text{O}_2\text{Cl}_3$, $\text{Ti}_2\text{O}_3\text{Cl}_2$, and

$\text{Ti}_2\text{O}_3\text{Cl}_3$, so although these are less stable than $\text{Ti}_2\text{O}_2\text{Cl}_4$ at most temperatures, they may still feature in a detailed kinetic mechanism, much like the lesser TiO_yCl_z species.

Of the many possible Ti_3 species, we expect $\text{Ti}_3\text{O}_4\text{Cl}_4$ to be one of the more stable due to the double-oxygen bridge between each of the Ti atoms. However, the equilibrium concentration of this species is predicted to be lower than that of the dimer by at least an order of magnitude. This implies that the critical nucleus size, above which molecules grow irreversibly and can be safely treated as particles[36], is larger than Ti_2 .

Below ~ 600 K the largest species in our simulation, $\text{Ti}_5\text{O}_6\text{Cl}_8$, is predicted to have the highest concentration of the species containing titanium. This suggests that at low temperatures the critical nucleus size has five or fewer Ti atoms. However, at the high temperatures employed to speed the kinetics in the industrial process, the Ti_5 species is unstable relative to the reactants $\text{TiCl}_4 + \text{O}_2$, suggesting that the critical nucleus size is even larger under those conditions.

4 Conclusion

Quantum calculations were used to obtain thermochemical data, including standard entropies and enthalpies of formation, for some titanium oxychloride species, $\text{Ti}_x\text{O}_y\text{Cl}_z$, many of which were not previously reported in the literature and are impossible to obtain with the available experimental techniques. These thermochemical data will enable the development of more detailed kinetic models of the combustion of titanium tetrachloride to produce titanium dioxide. A comparison of the results from these calculations with the NIST and JANAF tables suggests that the literature values for TiOCl_2 should be revised.

5 Acknowledgements

The authors would like to thank the EPSRC and Huntsman Tioxide for the financial support of RHW through an Industrial CASE studentship. Additional financial support from the US National Science Foundation is gratefully acknowledged. WHG thanks Churchill College for a Bye-Fellowship which greatly facilitated this collaboration.

References

- [1] Adamo, C. and Barone, V. (1998). Exchange functionals with improved long-range behavior and adiabatic connection methods without adjustable parameters: The mPW and mPW1PW models, *J. Chem. Phys.* **108**(2): 664–675.
- [2] Albaret, T., Finocchi, F. and Noguera, C. (2000). Density functional study of stoichiometric and O-rich titanium oxygen clusters, *J. Chem. Phys.* **113**: 2238–2249.
- [3] Becke, A. D. (1988). Density-functional exchange-energy approximation with correct asymptotic-behavior, *Phys. Rev. A* **38**(6): 3098–3100.
- [4] Becke, A. D. (1993). Density-functional thermochemistry. iii. the role of exact exchange, *J. Chem. Phys.* **98**(7): 5648–5651.
- [5] Binkley, J. S., Pople, J. A. and Hehre, W. J. (1980). Self-consistent molecular orbital methods. 21. small split-valence basis sets for first-row elements, *J. Am. Chem. Soc.* **102**(3): 939–947.
- [6] Boese, A. D., Martin, J. M. L. and Handy, N. C. (2003). The role of the basis set: Assessing density functional theory, *J. Chem. Phys.* **119**(6): 3005–3014.
- [7] Chase Jr., M. W. (1998). NIST-JANAF thermochemical tables, fourth edition, *J. Phys. Chem. Ref. Data.*
- [8] Frisch, M. J., Trucks, G. W., Schlegel, H. B., Scuseria, G. E., Robb, M. A., Cheeseman, J. R., Montgomery, Jr., J. A., Vreven, T., Kudin, K. N., Burant, J. C., Millam, J. M., Iyengar, S. S., Tomasi, J., Barone, V., Mennucci, B., Cossi, M., Scalmani, G., Rega, N., Petersson, G. A., Nakatsuji, H., Hada, M., Ehara, M., Toyota, K., Fukuda, R., Hasegawa, J., Ishida, M., Nakajima, T., Honda, Y., Kitao, O., Nakai, H., Klene, M., Li, X., Knox, J. E., Hratchian, H. P., Cross, J. B., Bakken, V., Adamo, C., Jaramillo, J., Gomperts, R., Stratmann, R. E., Yazyev, O., Austin, A. J., Cammi, R., Pomelli, C., Ochterski, J. W., Ayala, P. Y., Morokuma, K., Voth, G. A., Salvador, P., Dannenberg, J. J., Zakrzewski, V. G., Dapprich, S., Daniels, A. D., Strain, M. C., Farkas, O., Malick, D. K., Rabuck, A. D., Raghavachari, K., Foresman, J. B., Ortiz, J. V., Cui, Q., Baboul, A. G., Clifford, S., Cioslowski, J., Stefanov, B. B., Liu, G., Liashenko, A., Piskorz, P., Komaromi, I., Martin, R. L., Fox, D. J., Keith, T., Al-Laham, M. A., Peng, C. Y., Nanayakkara, A., Challacombe, M., Gill, P. M. W., Johnson, B., Chen, W., Wong, M. W., Gonzalez, C. and Pople, J. A. (2003). Gaussian 03, Revision C.02. Gaussian, Inc., Wallingford, CT, 2004.
- [9] Goodwin, D. G. (2003). An open source, extensible software suite for CVD process simulation, in M. Allendorff, F. Maury and F. Teyssandier (eds), *Chemical Vapor Deposition XVI and EUROCVD 14*, Vol. 2003-08 of *ECS Proceedings*, The Electrochemical Society, The Electrochemical Society, Pennington, New Jersey, USA, pp. 155–162.

- [10] Gordon, M. S., Binkley, J. S., Pople, J. A., Pietro, W. J. and Hehre, W. J. (1982). Self-consistent molecular-orbital methods. 22. small split-valence basis sets for second-row elements, *J. Am. Chem. Soc.* **104**(10): 2792–2803.
- [11] Gordon, S. and McBride, B. J. (1971). Computer program for calculation of complex chemical equilibrium composition, rocket performance, incident and reflected shocks and chapman-jouguet detonations, *Technical Report SP-273*, NASA.
- [12] Graham, D., Beran, G., Head-Gordon, M., Christian, G., Stranger, R. and Yates, B. (2005). Nitrogen activation via three-coordinate molybdenum complexes: Comparison of density functional theory performance with wave function based methods, *J. Phys. Chem. A* **109**(30): 6762–6772.
- [13] Guest, M., Bush, I. J., van Dam, H., Sherwood, P., Thomas, J., van Lenthe, J., Havenith, R. and Kendrick, J. (2005). The GAMESS-UK electronic structure package: algorithms, developments and applications, *Molecular Physics* **103**(6–8): 719–747.
- [14] Hamprecht, F. A., Cohen, A. J., Tozer, D. J. and Handy, N. C. (1998). Development and assessment of new exchange-correlation functionals, *J. Chem. Phys.* **109**(15): 6264–6271.
- [15] Hay, P. J. (1977). Gaussian basis sets for molecular calculations - representation of 3d orbitals in transition-metal atoms, *J. Chem. Phys.* **66**: 4377–4384.
- [16] Hay, P. J. and Wadt, W. R. (1985). Ab initio effective core potentials for molecular calculations. potentials for the transition metal atoms Sc to Hg, *J. Chem. Phys.* **82**(1): 270–283.
- [17] Hehre, W. J., Ditchfield, R., Radom, L. and Pople, J. A. (1970). Molecular orbital theory of the electronic structure of organic compounds. v. molecular theory of bond separation, *J. Am. Chem. Soc.* **92**(16): 4796–4801.
- [18] Hildenbrand, D. L. (1996). Thermochemical properties of gaseous $TiCl$, $TiCl_2$, and $TiCl_3$, *High. Temp. Mat. Sci.* **35**: 151–158.
- [19] Hildenbrand, D. L., Lau, K. H. and Mastrangelo, S. V. R. (1991). Gaseous species in the Ti-Al-Cl system and reaction with H_2O , *J. Phys. Chem.* **95**: 3435–3437.
- [20] Jeong, K. S., Chang, C., Sedlmayr, E. and Sulzle, D. (2000). Electronic structure investigation of neutral titanium oxide molecules tioxoy, *J. Phys. B-atomic Mol. Opt. Phys.* **33**: 3417–3430.
- [21] Karlemo, B., Koukkari, P. and Paloniemi, J. (1996). Formation of gaseous intermediates in titanium(IV) chloride plasma oxidation, *Plasma Chem. Plasma Processing* **16**: 59–77.
- [22] Krishnan, R., Binkley, J. S., Seeger, R. and Pople, J. A. (1980). Self-consistent molecular-orbital methods. 20. basis set for correlated wave-functions, *J. Chem. Phys.* **72**: 650–654.

- [23] Lee, T., Rice, J. and Rendell, A. (1991). The TITAN set of electronic structure programs.
- [24] McBride, B. J., Gordon, S. and Reno, M. A. (1993). Coefficients for calculating thermodynamic and transport properties of individual species, *Technical Report TM-4513*, NASA.
- [25] McLean, A. D. and Chandler, G. S. (1980). Contracted gaussian-basis sets for molecular calculations. 1. 2nd row atoms, z=11-18, *J. Chem. Phys.* **72**: 5639–5648.
- [26] Miller, J. A. and Bowman, C. T. (1989). Mechanism and modelling of nitrogen chemistry in combustion, *Prog. Energy Comust. Sci.* **15**: 287–338.
- [27] NIST (2005). Computational chemistry comparison and benchmark database.
- [28] Perdew, J. P., Chevary, J. A., Vosko, S. H., Jackson, K. A., Pederson, M. R., Singh, D. J. and Fiolhais, C. (1992). Atoms, molecules, solids, and surfaces: Applications of the generalized gradient approximation for exchange and correlation, *Phys. Rev. B* **46**(11): 6671–6687.
- [29] Perdew, J. P., Chevary, J. A., Vosko, S. H., Jackson, K. A., Pederson, M. R., Singh, D. J. and Fiolhais, C. (1993). Erratum: Atoms, molecules, solids, and surfaces: Applications of the generalized gradient approximation for exchange and correlation, *Phys. Rev. B* **48**(7): 4978.
- [30] Pople, J. A. and Curtiss, L. A. (1987). Theoretical thermochemistry. 3. a modified procedure for ionization energies of AH_n species, *J. Phys. Chem.* **91**(13): 3637–3639.
- [31] Pople, J. A., Luke, B. T., Frisch, M. J. and Binkley, J. S. (1985). Theoretical thermochemistry. 1. heats of formation of neutral AH_n molecules ($A = Li$ to Cl), *J. Phys. Chem.* **89**(11): 2198–2203.
- [32] Pratsinis, S. E., Bai, H., Biswas, P., Frenklach, M. and Mastrangelo, S. V. R. (1990). Kinetics of titanium(IV) chloride oxidation, *J. Am. Ceram. Soc.* **73**: 2158–2162.
- [33] Raghavachari, K. and Trucks, G. W. (1989). Highly correlated systems - excitation-energies of 1st row transition-metals Sc-Cu, *J. Chem. Phys.* **91**: 1062–1065.
- [34] Scott, A. P. and Radom, L. (1996). Harmonic vibrational frequencies: An evaluation of Hartree-Fock, Moller-Plesset, quadratic configuration interaction, density functional theory, and semiempirical scale factors, *J. Phys. Chem.* **100**: 16502–16513.
- [35] Wachters, A. J. (1970). Gaussian basis set for molecular wavefunctions containing third-row atoms, *J. Chem. Phys.* **52**: 1033–1036.
- [36] Wong, H. W., Li, X. G., Swihart, M. T. and Broadbelt, L. J. (2004). Detailed kinetic modeling of silicon nanoparticle formation chemistry via automated mechanism generation, *J. Phys. Chem. A* **108**: 10122–10132.

- [37] Woodley, S. M., Hamad, S., Mejias, J. A. and Catlow, C. R. A. (2006). Properties of small TiO₂, ZrO₂ and HfO₂ nanoparticles, *J. Mater. Chem.* **16**: 1927–1933.

6 Appendices

Thermochemical tables and polynomial coefficients in NASA form, formatted for Cantera software[9], for $C_p(T)$, $H^\circ(T)$ and $S^\circ(T)$ are available for the species TiOCl, TiOCl₂, TiOCl₃, TiO₂Cl₂, TiO₂Cl₃, Ti₂O₃Cl₃, Ti₂O₃Cl₂, Ti₂O₂Cl₃, Ti₃O₄Cl₄, Ti₂O₂Cl₄, and Ti₅O₆Cl₈.

If viewing this document in Adobe Acrobat Reader, the full mechanism in Cantera format can be extracted by clicking on this paperclip:



Table 5: *TiOCl thermochemistry*

T (K)	C _p (J/mol/K)	H (kJ/mol)	S (J/mol/K)
100	40.86	-283.51	242.76
150	43.63	-281.39	259.88
200	45.77	-279.16	272.73
250	47.52	-276.82	283.14
298.15	48.96	-274.50	291.64
300	49.01	-274.41	291.94
350	50.30	-271.93	299.60
400	51.41	-269.38	306.39
450	52.34	-266.79	312.50
500	53.12	-264.15	318.05
600	54.33	-258.77	327.85
700	55.18	-253.30	336.29
800	55.79	-247.75	343.70
900	56.24	-242.14	350.30
1000	56.58	-236.50	356.25
1100	56.84	-230.83	361.65
1200	57.04	-225.14	366.61
1300	57.20	-219.42	371.18
1400	57.34	-213.70	375.42
1500	57.44	-207.96	379.38
1600	57.53	-202.21	383.09
1700	57.60	-196.45	386.58
1800	57.67	-190.69	389.88
1900	57.72	-184.92	393.00
2000	57.77	-179.14	395.96
2100	57.81	-173.37	398.78
2200	57.84	-167.58	401.47
2300	57.87	-161.80	404.04
2400	57.90	-156.01	406.50
2500	57.92	-150.22	408.87
2600	57.94	-144.43	411.14
2700	57.96	-138.63	413.33
2800	57.98	-132.83	415.43
2900	57.99	-127.03	417.47
3000	58.01	-121.24	419.44

Table 6: *TiOCl₂ thermochemistry*

T (K)	C _p (J/mol/K)	H (kJ/mol)	S (J/mol/K)
100	53.63	-610.53	267.83
150	59.70	-607.69	290.78
200	64.20	-604.58	308.60
250	67.54	-601.28	323.30
298.15	70.03	-597.97	335.42
300	70.12	-597.84	335.86
350	72.17	-594.28	346.82
400	73.83	-590.63	356.57
450	75.18	-586.90	365.35
500	76.28	-583.12	373.33
600	77.95	-575.40	387.39
700	79.10	-567.54	399.50
800	79.93	-559.59	410.12
900	80.53	-551.57	419.57
1000	80.99	-543.49	428.08
1100	81.33	-535.37	435.82
1200	81.61	-527.22	442.91
1300	81.82	-519.05	449.45
1400	82.00	-510.86	455.52
1500	82.14	-502.65	461.18
1600	82.26	-494.43	466.49
1700	82.35	-486.20	471.47
1800	82.44	-477.96	476.18
1900	82.51	-469.72	480.64
2000	82.57	-461.46	484.88
2100	82.62	-453.20	488.91
2200	82.67	-444.94	492.75
2300	82.71	-436.67	496.43
2400	82.74	-428.40	499.95
2500	82.77	-420.12	503.33
2600	82.80	-411.84	506.57
2700	82.83	-403.56	509.70
2800	82.85	-395.28	512.71
2900	82.87	-386.99	515.62
3000	82.89	-378.70	518.43

Table 7: *TiOCl₃ thermochemistry*

T (K)	C _p (J/mol/K)	H (kJ/mol)	S (J/mol/K)
100	67.99	-655.79	290.45
150	77.85	-652.13	319.98
200	85.35	-648.04	343.45
250	90.84	-643.63	363.12
298.15	94.65	-639.16	379.46
300	94.77	-638.98	380.05
350	97.60	-634.17	394.88
400	99.67	-629.24	408.06
450	101.20	-624.21	419.89
500	102.37	-619.12	430.62
600	103.98	-608.80	449.43
700	105.01	-598.35	465.55
800	105.70	-587.81	479.62
900	106.18	-577.21	492.10
1000	106.53	-566.58	503.30
1100	106.80	-555.91	513.47
1200	107.00	-545.22	522.77
1300	107.16	-534.51	531.34
1400	107.28	-523.79	539.29
1500	107.39	-513.06	546.69
1600	107.47	-502.31	553.63
1700	107.54	-491.56	560.14
1800	107.60	-480.80	566.29
1900	107.65	-470.04	572.11
2000	107.69	-459.27	577.63
2100	107.73	-448.50	582.89
2200	107.76	-437.73	587.90
2300	107.79	-426.95	592.69
2400	107.81	-416.17	597.28
2500	107.83	-405.39	601.68
2600	107.85	-394.61	605.91
2700	107.87	-383.82	609.98
2800	107.89	-373.03	613.90
2900	107.90	-362.24	617.69
3000	107.91	-351.45	621.35

Table 8: *TiO₂Cl₂ thermochemistry*

T (K)	C _p (J/mol/K)	H (kJ/mol)	S (J/mol/K)
100	58.68	-572.69	263.76
150	67.72	-569.52	289.34
200	75.11	-565.94	309.87
250	81.24	-562.03	327.31
298.15	86.01	-558.00	342.04
300	86.18	-557.84	342.58
350	90.07	-553.43	356.16
400	93.14	-548.85	368.40
450	95.55	-544.13	379.52
500	97.47	-539.30	389.69
600	100.25	-529.40	407.72
700	102.10	-519.28	423.32
800	103.38	-509.00	437.04
900	104.30	-498.62	449.28
1000	104.98	-488.15	460.30
1100	105.49	-477.63	470.33
1200	105.89	-467.06	479.53
1300	106.20	-456.45	488.02
1400	106.46	-445.82	495.90
1500	106.66	-435.16	503.25
1600	106.83	-424.49	510.14
1700	106.97	-413.80	516.62
1800	107.09	-403.10	522.74
1900	107.19	-392.38	528.53
2000	107.28	-381.66	534.03
2100	107.35	-370.93	539.27
2200	107.41	-360.19	544.26
2300	107.47	-349.44	549.04
2400	107.52	-338.69	553.61
2500	107.57	-327.94	558.00
2600	107.60	-317.18	562.22
2700	107.64	-306.42	566.28
2800	107.67	-295.65	570.20
2900	107.70	-284.88	573.98
3000	107.72	-274.11	577.63

Table 9: *TiO₂Cl₃ thermochemistry*

T (K)	C _p (J/mol/K)	H (kJ/mol)	S (J/mol/K)
100	74.60	-792.77	302.17
150	87.94	-788.69	335.05
200	98.01	-784.03	361.81
250	105.26	-778.94	384.50
298.15	110.35	-773.74	403.50
300	110.52	-773.54	404.18
350	114.45	-767.91	421.53
400	117.46	-762.11	437.02
450	119.84	-756.17	450.99
500	121.73	-750.13	463.72
600	124.52	-737.81	486.18
700	126.43	-725.25	505.53
800	127.79	-712.54	522.50
900	128.78	-699.71	537.62
1000	129.52	-686.79	551.22
1100	130.08	-673.81	563.60
1200	130.52	-660.78	574.93
1300	130.87	-647.71	585.40
1400	131.16	-634.61	595.11
1500	131.39	-621.48	604.16
1600	131.58	-608.33	612.65
1700	131.74	-595.17	620.63
1800	131.88	-581.98	628.16
1900	131.99	-568.79	635.30
2000	132.09	-555.59	642.07
2100	132.18	-542.37	648.52
2200	132.25	-529.15	654.67
2300	132.32	-515.92	660.55
2400	132.37	-502.69	666.18
2500	132.42	-489.45	671.59
2600	132.47	-476.20	676.78
2700	132.51	-462.95	681.78
2800	132.55	-449.70	686.60
2900	132.58	-436.45	691.25
3000	132.61	-423.19	695.75

Table 10: $Ti_2O_2Cl_3$ thermochemistry

T (K)	C_p (J/mol/K)	H (kJ/mol)	S (J/mol/K)
100	82.43	-1278.72	323.50
150	98.20	-1274.19	360.01
200	111.14	-1268.95	390.10
250	121.26	-1263.13	416.03
298.15	128.70	-1257.10	438.06
300	128.94	-1256.86	438.85
350	134.70	-1250.26	459.18
400	139.04	-1243.42	477.47
450	142.35	-1236.38	494.04
500	144.90	-1229.19	509.18
600	148.49	-1214.51	535.94
700	150.81	-1199.54	559.02
800	152.39	-1184.37	579.26
900	153.51	-1169.07	597.28
1000	154.32	-1153.68	613.50
1100	154.94	-1138.22	628.24
1200	155.41	-1122.70	641.74
1300	155.78	-1107.14	654.20
1400	156.08	-1091.54	665.75
1500	156.32	-1075.92	676.53
1600	156.51	-1060.28	686.62
1700	156.68	-1044.62	696.12
1800	156.82	-1028.95	705.08
1900	156.93	-1013.26	713.56
2000	157.04	-997.56	721.61
2100	157.12	-981.85	729.27
2200	157.20	-966.14	736.59
2300	157.26	-950.41	743.57
2400	157.32	-934.68	750.27
2500	157.37	-918.95	756.69
2600	157.42	-903.21	762.87
2700	157.46	-887.47	768.81
2800	157.49	-871.72	774.53
2900	157.53	-855.97	780.06
3000	157.56	-840.21	785.40

Table 11: $Ti_2O_2Cl_4$ thermochemistry

T (K)	C_p (J/mol/K)	H (kJ/mol)	S (J/mol/K)
100	93.52	-1577.12	317.09
150	112.78	-1571.94	358.79
200	128.29	-1565.90	393.45
250	140.27	-1559.17	423.42
298.15	148.98	-1552.20	448.91
300	149.27	-1551.92	449.83
350	155.99	-1544.28	473.37
400	161.03	-1536.35	494.55
450	164.86	-1528.20	513.75
500	167.82	-1519.88	531.27
600	171.97	-1502.88	562.27
700	174.66	-1485.54	588.99
800	176.48	-1467.97	612.44
900	177.77	-1450.26	633.31
1000	178.71	-1432.43	652.09
1100	179.42	-1414.52	669.15
1200	179.96	-1396.55	684.79
1300	180.39	-1378.54	699.21
1400	180.73	-1360.48	712.59
1500	181.01	-1342.39	725.07
1600	181.23	-1324.28	736.76
1700	181.42	-1306.15	747.75
1800	181.58	-1288.00	758.13
1900	181.72	-1269.83	767.95
2000	181.84	-1251.65	777.27
2100	181.94	-1233.46	786.15
2200	182.02	-1215.27	794.61
2300	182.10	-1197.06	802.71
2400	182.16	-1178.85	810.46
2500	182.22	-1160.63	817.90
2600	182.28	-1142.40	825.04
2700	182.32	-1124.17	831.92
2800	182.36	-1105.94	838.55
2900	182.40	-1087.70	844.95
3000	182.43	-1069.46	851.14

Table 12: $Ti_2O_3Cl_2$ thermochemistry

T (K)	C_p (J/mol/K)	H (kJ/mol)	S (J/mol/K)
100	73.73	-1350.67	296.10
150	90.10	-1346.56	329.21
200	103.28	-1341.72	357.00
250	113.79	-1336.28	381.22
298.15	121.77	-1330.60	401.98
300	122.04	-1330.37	402.73
350	128.48	-1324.10	422.05
400	133.50	-1317.55	439.55
450	137.45	-1310.77	455.51
500	140.57	-1303.82	470.16
600	145.11	-1289.52	496.22
700	148.13	-1274.85	518.83
800	150.23	-1259.92	538.75
900	151.74	-1244.82	556.54
1000	152.85	-1229.59	572.59
1100	153.70	-1214.26	587.20
1200	154.35	-1198.86	600.60
1300	154.87	-1183.39	612.97
1400	155.28	-1167.88	624.47
1500	155.62	-1152.34	635.19
1600	155.90	-1136.76	645.24
1700	156.13	-1121.16	654.70
1800	156.33	-1105.54	663.63
1900	156.49	-1089.90	672.09
2000	156.63	-1074.24	680.12
2100	156.76	-1058.57	687.77
2200	156.86	-1042.89	695.06
2300	156.96	-1027.20	702.04
2400	157.04	-1011.50	708.72
2500	157.11	-995.79	715.13
2600	157.18	-980.08	721.29
2700	157.23	-964.35	727.23
2800	157.29	-948.63	732.95
2900	157.33	-932.90	738.47
3000	157.37	-917.16	743.80

Table 13: $Ti_2O_3Cl_3$ thermochemistry

T (K)	C_p (J/mol/K)	H (kJ/mol)	S (J/mol/K)
100	93.58	-1442.59	330.06
150	112.52	-1437.42	371.75
200	127.51	-1431.41	406.26
250	139.26	-1424.72	436.03
298.15	147.95	-1417.80	461.33
300	148.24	-1417.53	462.25
350	155.03	-1409.94	485.63
400	160.17	-1402.05	506.69
450	164.11	-1393.94	525.79
500	167.16	-1385.65	543.24
600	171.46	-1368.71	574.13
700	174.26	-1351.41	600.79
800	176.16	-1333.88	624.19
900	177.51	-1316.20	645.02
1000	178.50	-1298.39	663.78
1100	179.24	-1280.51	680.82
1200	179.81	-1262.55	696.45
1300	180.26	-1244.55	710.86
1400	180.62	-1226.50	724.23
1500	180.91	-1208.43	736.70
1600	181.15	-1190.32	748.38
1700	181.35	-1172.20	759.37
1800	181.51	-1154.06	769.74
1900	181.66	-1135.90	779.56
2000	181.78	-1117.72	788.88
2100	181.88	-1099.54	797.75
2200	181.98	-1081.35	806.22
2300	182.05	-1063.15	814.31
2400	182.12	-1044.94	822.06
2500	182.19	-1026.72	829.49
2600	182.24	-1008.50	836.64
2700	182.29	-990.27	843.52
2800	182.33	-972.04	850.15
2900	182.37	-953.81	856.55
3000	182.41	-935.57	862.73

Table 14: $Ti_3O_4Cl_4$ thermochemistry

T (K)	C_p (J/mol/K)	H (kJ/mol)	S (J/mol/K)
100	119.31	-2333.52	364.74
150	147.02	-2326.84	418.53
200	170.04	-2318.90	464.08
250	188.41	-2309.92	504.09
298.15	202.09	-2300.50	538.49
300	202.55	-2300.13	539.75
350	213.29	-2289.72	571.81
400	221.45	-2278.84	600.85
450	227.71	-2267.60	627.31
500	232.56	-2256.09	651.56
600	239.42	-2232.47	694.62
700	243.89	-2208.29	731.89
800	246.93	-2183.74	764.66
900	249.09	-2158.93	793.88
1000	250.66	-2133.94	820.21
1100	251.85	-2108.81	844.16
1200	252.77	-2083.58	866.11
1300	253.48	-2058.26	886.37
1400	254.06	-2032.89	905.18
1500	254.53	-2007.46	922.72
1600	254.91	-1981.98	939.16
1700	255.23	-1956.48	954.63
1800	255.50	-1930.94	969.22
1900	255.73	-1905.38	983.04
2000	255.92	-1879.79	996.17
2100	256.09	-1854.19	1008.66
2200	256.24	-1828.58	1020.57
2300	256.36	-1802.95	1031.97
2400	256.48	-1777.31	1042.88
2500	256.58	-1751.65	1053.35
2600	256.66	-1725.99	1063.42
2700	256.74	-1700.32	1073.10
2800	256.81	-1674.64	1082.44
2900	256.88	-1648.96	1091.46
3000	256.93	-1623.27	1100.17

Table 15: $Ti_5O_6Cl_8$ thermochemistry

T (K)	C_p (J/mol/K)	H (kJ/mol)	S (J/mol/K)
100	220.67	-4071.44	502.51
150	273.23	-4059.04	602.33
200	314.21	-4044.31	686.81
250	345.17	-4027.78	760.42
298.15	367.57	-4010.60	823.22
300	368.31	-4009.92	825.50
350	385.65	-3991.05	883.64
400	398.75	-3971.42	936.03
450	408.78	-3951.23	983.60
500	416.57	-3930.58	1027.09
600	427.60	-3888.33	1104.09
700	434.80	-3845.19	1170.58
800	439.72	-3801.45	1228.98
900	443.20	-3757.29	1280.99
1000	445.76	-3712.84	1327.82
1100	447.69	-3668.16	1370.40
1200	449.18	-3623.32	1409.42
1300	450.35	-3578.34	1445.42
1400	451.28	-3533.25	1478.83
1500	452.04	-3488.09	1509.99
1600	452.67	-3442.85	1539.19
1700	453.19	-3397.56	1566.65
1800	453.62	-3352.22	1592.56
1900	454.00	-3306.83	1617.10
2000	454.31	-3261.42	1640.40
2100	454.59	-3215.97	1662.57
2200	454.83	-3170.50	1683.72
2300	455.04	-3125.01	1703.94
2400	455.22	-3079.50	1723.31
2500	455.38	-3033.97	1741.90
2600	455.52	-2988.42	1759.76
2700	455.65	-2942.86	1776.96
2800	455.77	-2897.29	1793.53
2900	455.87	-2851.71	1809.53
3000	455.96	-2806.12	1824.98

Table 16: Polynomial coefficients formatted for Cantera[9].

```

species(name = 'TiOCL', # ClOTi(2)
        atoms = 'Ti:1 O:1 Cl:1',
        thermo = (
            NASA( [ 100.00, 1000.00], [ 4.191335334e+000 , 8.594198813e-003 , -1.194247195e-005 ,
                  8.231298290e-009 , -2.269569234e-012 , -3.455624647e+004 , 9.094304222e+000 ] ),
            NASA( [ 1000.00, 3000.00], [ 6.022828351e+000 , 1.426477358e-003 , -8.569483759e-007 ,
                  2.374434516e-010 , -2.500952595e-014 , -3.494901354e+004 , 1.712366899e-001 ] )
        )
    )
species(name = 'TiOCL2', # Cl2OTi
        atoms = 'Ti:1 O:1 Cl:2',
        thermo = (
            NASA( [ 100.00, 1000.00], [ 4.850999861e+000 , 2.001354777e-002 , -3.465798181e-005 ,
                  2.844112110e-008 , -8.907190590e-012 , -7.400245633e+004 , 8.038481407e+000 ] ),
            NASA( [ 1000.00, 3000.00], [ 8.952753228e+000 , 1.304839902e-003 , -6.505917942e-007 ,
                  1.454512241e-010 , -1.195622092e-014 , -7.478660155e+004 , -1.138233284e+001 ] )
        )
    )
species(name = 'TiOCL3', # Cl3OTi(2)
        atoms = 'Ti:1 O:1 Cl:3',
        thermo = (
            NASA( [ 100.00, 1000.00], [ 5.303769917e+000 , 3.609899817e-002 , -6.891844111e-005 ,
                  5.933749393e-008 , -1.900887435e-011 , -7.956110654e+004 , 7.229069323e+000 ] ),
            NASA( [ 1000.00, 3000.00], [ 1.255201104e+001 , 2.083186728e-004 , 1.458171831e-007 ,
                  -1.119486595e-010 , 1.874831780e-014 , -8.082008753e+004 , -2.642188101e+001 ] )
        )
    )
species(name = 'TiO2CL2', # Cl2O2Ti
        atoms = 'Ti:1 O:2 Cl:2',
        thermo = (
            NASA( [ 100.00, 1000.00], [ 4.262345042e+000 , 3.311452396e-002 , -5.408385407e-005 ,
                  4.165517914e-008 , -1.232245038e-011 , -6.945311454e+004 , 9.040953840e+000 ] ),
            NASA( [ 1000.00, 3000.00], [ 1.117107315e+001 , 2.614342668e-003 , -1.529401279e-006 ,
                  4.119050053e-010 , -4.217585084e-014 , -7.077267466e+004 , -2.378220491e+001 ] )
        )
    )
species(name = 'TiO2CL3', # Cl3O2Ti(2)
        atoms = 'Ti:1 O:2 Cl:3',
        thermo = (
            NASA( [ 100.00, 1000.00], [ 5.269306207e+000 , 4.675346588e-002 , -8.716316859e-005 ,
                  7.471267398e-008 , -2.399527772e-011 , -9.607932393e+004 , 7.820210546e+000 ] ),
            NASA( [ 1000.00, 3000.00], [ 1.463673799e+001 , 1.321746381e-003 , -3.974673409e-007 ,
                  6.702843464e-012 , 9.279889448e-015 , -9.776532144e+004 , -3.593799597e+001 ] )
        )
    )
species(name = 'Ti2O2CL3', # Cl3O2Ti2(2)
        atoms = 'Ti:2 O:2 Cl:3',
        thermo = (
            NASA( [ 100.00, 1000.00], [ 4.931408223e+000 , 6.023515816e-002 , -1.077364926e-004 ,
                  8.860976031e-008 , -2.747908105e-011 , -1.545537194e+005 , 1.068794261e+001 ] ),
            NASA( [ 1000.00, 3000.00], [ 1.722666713e+001 , 2.183796225e-003 , -1.057418655e-006 ,
                  2.246625490e-010 , -1.695422095e-014 , -1.567700421e+005 , -4.693670453e+001 ] )
        )
    )
)

```

```

species(name = 'Ti2O2CL4', # Cl4O2Ti2
        atoms = 'Ti:2 O:2 Cl:4',
        thermo = (
            NASA( [ 100.00, 1000.00], [ 5.287928342e+000 , 7.264555733e-002 , -1.315418425e-004 ,
                1.092099731e-007 , -3.410813206e-011 , -1.905322783e+005 , 7.148863410e+000 ] ),
            NASA( [ 1000.00, 3000.00], [ 2.007576714e+001 , 2.235305708e-003 , -9.861436133e-007 ,
                1.779749240e-010 , -9.419976711e-015 , -1.931830502e+005 , -6.205018457e+001 ] )
        )
    )

species(name = 'Ti2O3CL2', # Cl2O3Ti2
        atoms = 'Ti:2 O:3 Cl:2',
        thermo = (
            NASA( [ 100.00, 1000.00], [ 3.909075052e+000 , 5.965984584e-002 , -1.014950910e-004 ,
                8.092530048e-008 , -2.461517124e-011 , -1.631042851e+005 , 1.212928629e+001 ] ),
            NASA( [ 1000.00, 3000.00], [ 1.623336441e+001 , 3.733781124e-003 , -2.049869971e-006 ,
                5.158950596e-010 , -4.921153511e-014 , -1.654173822e+005 , -4.613878918e+001 ] )
        )
    )

species(name = 'Ti2O3CL3', # Cl3O3Ti2(2)
        atoms = 'Ti:2 O:3 Cl:3',
        thermo = (
            NASA( [ 100.00, 1000.00], [ 5.505996743e+000 , 7.001288499e-002 , -1.246293063e-004 ,
                1.022487306e-007 , -3.167024157e-011 , -1.743635689e+005 , 7.935704258e+000 ] ),
            NASA( [ 1000.00, 3000.00], [ 1.983763106e+001 , 2.680484415e-003 , -1.311081065e-006 ,
                2.829445581e-010 , -2.191453749e-014 , -1.769626336e+005 , -5.931391681e+001 ] )
        )
    )

species(name = 'Ti3O4CL4', # Cl4O4Ti3
        atoms = 'Ti:3 O:4 Cl:4',
        thermo = (
            NASA( [ 100.00, 1000.00], [ 5.479788968e+000 , 1.062529189e-001 , -1.860208915e-004 ,
                1.506020848e-007 , -4.616620602e-011 , -2.816765321e+005 , 8.893090485e+000 ] ),
            NASA( [ 1000.00, 3000.00], [ 2.728670412e+001 , 4.878072197e-003 , -2.581765180e-006 ,
                6.207116407e-010 , -5.602761069e-014 , -2.856556257e+005 , -9.362221280e+001 ] )
        )
    )

species(name = 'Ti5O6CL8', # Cl8O6Ti5
        atoms = 'Ti:5 O:6 Cl:8',
        thermo = (
            NASA( [ 100.00, 1000.00], [ 1.099206826e+001 , 1.918922127e-001 , -3.501070247e-004 ,
                2.929909361e-007 , -9.215555300e-011 , -4.916228702e+005 , -7.694731180e+000 ] ),
            NASA( [ 1000.00, 3000.00], [ 5.001821678e+001 , 5.456972688e-003 , -2.162428702e-006 ,
                3.028700143e-010 , -2.991440285e-015 , -4.986346615e+005 , -1.902903243e+002 ] )
        )
    )
)

```